Size Matters: Be Wary of Characterizing Aerosol Composition and Type with Pseudo-Intrinsic Parameters

Gregory.L.Schuster@nasa.gov, NASA Langley Research Center, Hampton, Virginia
Oleg Dubovik, Antti Arola, Tom Eck, and Brent Holben

Word	Definitions	**Aerosol Examples**
Intrinsic (or intensive)	independent of mass	Refractive Index
Extrinsic (or extensive)	dependent upon mass	AOD, AAOD, etc.
Pseudo-Intrinsic	independent of mass, but sensitive to size.	SSA, AAE, Lidar Ratio, etc.

The AAE approach for speciating absorbers

Separate absorption AOD into carbon and dust components:

$$AERONET\ AAOD = C\lambda^{-AAE} = C_{dust}\lambda^{-AAE_d} + C_{BC}\lambda^{-AAE_{BC}} + C_{BrC}\lambda^{-AAE_{BrC}}$$

where the exponents are from climatology:

$AAE_{dust} = 2.4$ Pure Dust
$AAE_{carbon} \simeq 1$ Carbonaceous (0.84 to 1.16, depending upon region)
$AAE_{BC} = 0.5$ Pure Black Carbon
$AAE_{BrC} = 4.8$ Brown Carbon

Multiple wavelengths → Multiple equations, and can solve for coefficients C_i

Problems with the AAE approach:

1. Assumes AAE is independent of size.
2. It does not account for the variability in the AAE of dust (0 to 3.5).
3. Replaces AERONET internal mixture with external mixtures.

The AAE approach assumes that component aerosol absorption can be represented with component power laws. This is equivalent to assuming that all absorbing aerosols are externally mixed with one another and that the AAE is independent of size. This is inconsistent with the AERONET assumptions that are used to retrieve the AAOD and AAE. Thus, the link to the measured radiances is broken with this approach.

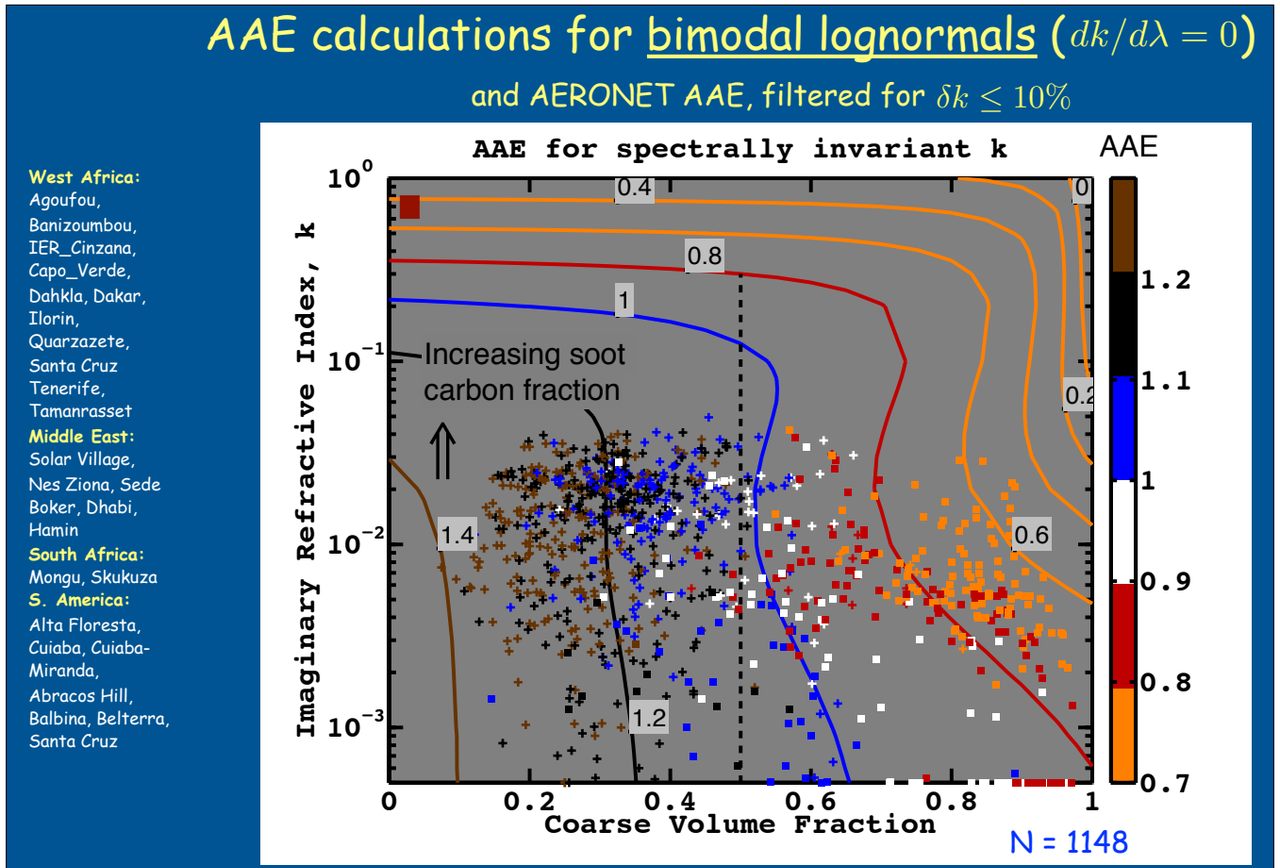

From Schuster et al (ACP, 2016, part 2).
Contours represent the AAE calculated for a bimodal aerosol size distribution of spherical particles that have a constant imaginary refractive index (IRI) wrt wavelength. This equivalently represents internal mixtures of black carbon with a non-absorbing host; increasing the imaginary refractive index represents increasing BC fractions. The maroon square represents the AAE that is obtained using pure black carbon with refractive indices in the range recommended by Bond and Bergstrom (AST, 2006). If retrievals were available in this range of refractive indices they would have good sensitivity to AAE, as the AAE contours are orthogonal to the y-axis. However, AERONET refractive indices do not reach these high values because external mixtures are essentially required to produce such high IRI, and the AERONET retrievals assume that all aerosols are internally mixed.

Data are AAE (440–870) at the AERONET sites, filtered for a maximum spectral variability in IRI of 10% with respect to the mean retrieved IRI. Biomass burning sites are “+” symbols, dust sites are squares. Note that the AAE contours are parallel to the y-axis in this range of refractive indices, which means that the AAE is not sensitive to the IRI (and equivalently, to the BC concentration). The contours are perpendicular to the coarse volume fraction, though, which indicates that the AAE is sensitive to size when IRI is low. Also note that the color of the AERONET data is consistent with the contours, indicating a consistency of the contours with the AERONET data.

Only 5% of the particles dominated by the fine mode indicate AAE < 1, but 90% of the particles dominated by the coarse mode indicate AAE < 1. Thus, AAE < 1 is more likely to represent coarse mode particles than fine mode BC.

Take-home message of this figure: AAE is much more sensitive to size than to IRI or BC fraction for the range of IRI provided by the AERONET database.

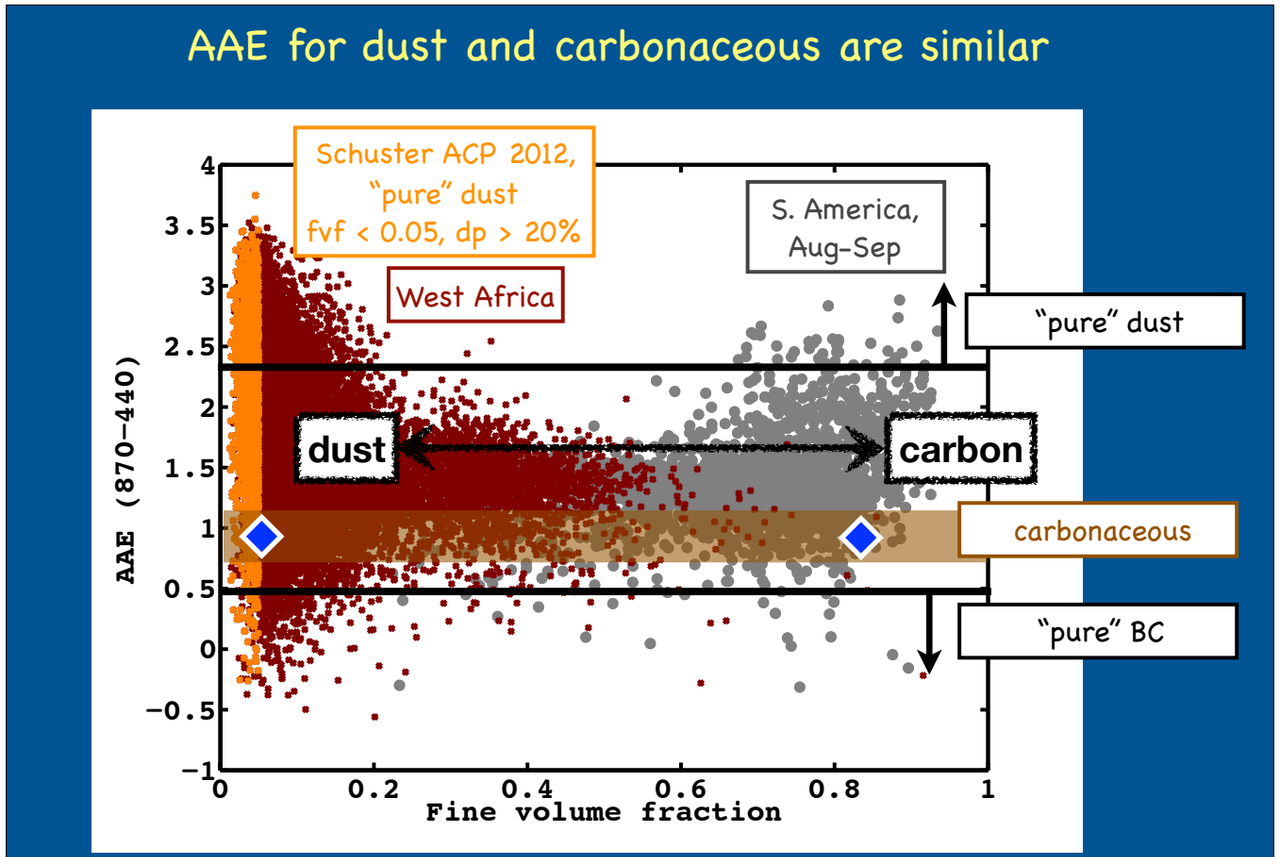

Absorption Angstrom exponent (AAE) vs. fine volume fraction during the South American biomass burning season (gray circles) and at the West African sites (maroon squares). Low Angstrom Exponents (AE) are located on the left, high AE on the right. The AAE approach locates all dust at the top of this plot and all carbonaceous near the bottom (denoted by text with smooth boxes). This is inconsistent with traditional approaches (denoted by black text with ragged boxes), which locate dust on the left side (low AE) and carbonaceous on the right side (high AE). Additionally, the AAE approach assigns the same component absorption to all particles with the same AAE. Thus, the two large blue diamonds have the exact same proportions of absorbing aerosols, despite one of the diamonds being composed of a very low fine volume fraction and high linear depolarization ratio, whereas the other diamond has a high fine volume fraction and is likely smoke.

From Schuster et al, ACP 2016, part 2.

We have Refractive Index – Why not use it?

Critics *Claim*: Result is sensitive to the inclusion refractive indices

Let's Test This

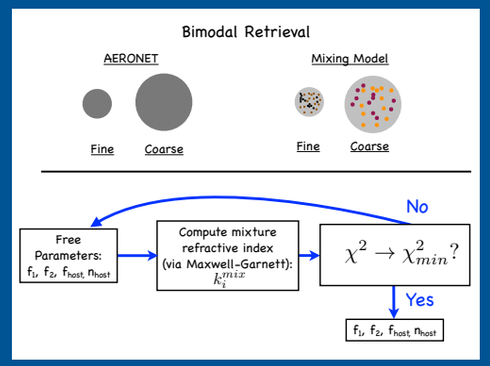

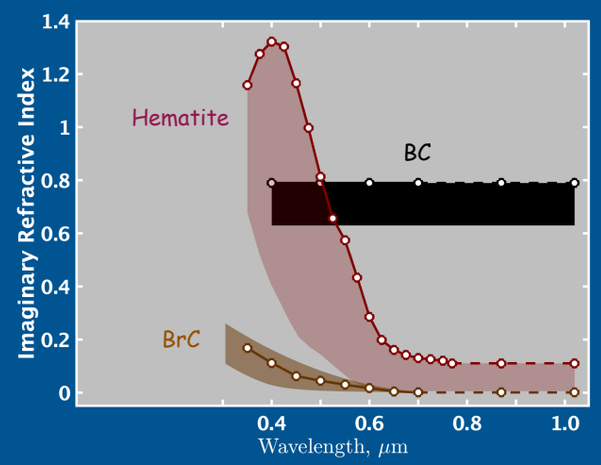

Different components in fine & coarse modes	
Fine Mode	Coarse Mode
Non-absorbing host	Non-absorbing host
black carbon	hematite
brown carbon	goethite
sometimes hematite	sometimes BC and BrC

Schuster (ACP, 2016, part 1)

Refractive Index Sources:
- Black Carbon:
  - Bond & Bergstrom (AST, 2006)
- Hematite:
  - Chen & Cahan (JOSA, 1981)
  - Gillespie & Lindberg (Appl. Optics., 1992)
  - Hsu & Matijevic (Appl. Optics., 1985)
- Brown Carbon:
  - Kirchstetter (JGR, 2004)
  - Sun (GRL, 2007)
  - Chen & Bond (ACP, 2010)

Refractive index approach is consistent with original AERONET retrieval. Critiques argue that the retrieval is sensitive to the complex refractive index of the absorbing components, so we test this for a large range of refractive indices here.

RESULTS

- Tested BC mass sensitivity to 24 combinations of component refractive indices at 14 AERONET sites in West Africa.
- Tested BC AAOD sensitivity to full range of black carbon refractive indices recommended by BB06 at 28 AERONET sites.
- Also computed AERONET $\delta AAOD$ uncertainty, assuming $\delta\omega = 0.03$ and $\delta AOD = 0.01$.

Less than 15% variability in BC

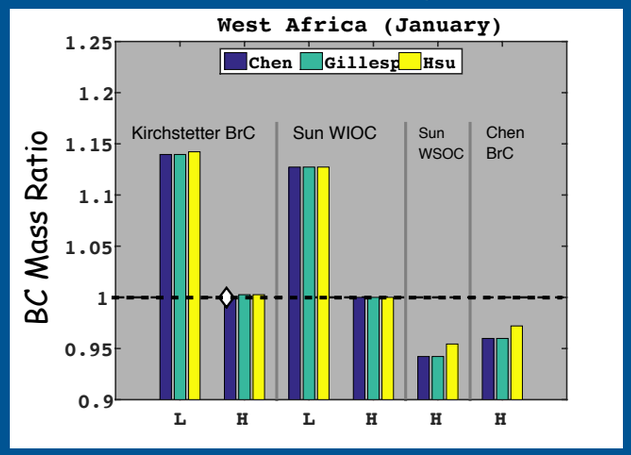

Schuster (ACP, 2016, part 1)

14 AERONET Sites:

Agoufou, Banizoumbou, IER_Cinzana, DMN_Maine_Soroa, Ouagadougou, Djougou, Saada, Capo_Verde, Dahkla, Dakar, Ilorin, Quarzazate, Santa_Cruz_Tenerife, Tamanrasset_INM, Tamanrasset_TMP

BC AAOD variability is less than measurement noise

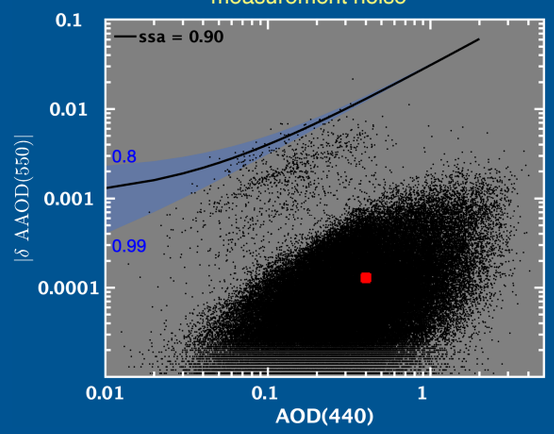

28 AERONET Sites:

Agoufou, Banizoumbou, IER_Cinzana, DMN_Maine_Soroa, Ouagadougou, Djougou, Saada, Capo_Verde, Dahkla, Dakar, Ilorin, Quarzazate, Tamanrasset_INM, Tamanrasset_TMP, Solar_Village, Nes_Ziona, SEDE_BOKER, Dhabi, Hamim, Mongu, Skukuza, Belterra, SANTA_CRUZ, Alta_Floresta, Cuiaba, CUIABA-MIRANDA, Abracos_Hill, Balbina

The results of our sensitivity studies indicate that the BC mass fraction and BC volume fraction changes by at most 14.2% for the range of inclusion refractive indices provided on the previous slide (left plot: [BC ratio = (BC fraction retrieved with base refractive index) / (BC fraction retrieved with alternate refractive index)]. Subsequent to the Schuster ACP 2016 papers, modelers have requested BC AAOD, which we have computed and provided online at https://science.larc.nasa.gov/personal-pages/gregs/data/2019-08-26/ . We also repeated our sensitivity test for the range of BC refractive indices recommended by Bond and Bergstrom (AST 2006), which are shown by the black dots on the right slide (red square is average of black dots). The black line and blue shaded area are the estimated AAOD uncertainty in the AERONET retrievals. The vast majority of the black dots are located below the estimated AERONET AAOD uncertainty, indicating that our technique does not have significant sensitivity to the refractive index of the absorbing inclusions. The reason for this is because the retrieval uses the retrieved refractive index as a constraint; thus, a lower BC refractive index for the inclusions results in a 14.2% increase in the BC volume fraction (previous slide), but the BC contribution to the IRI remains essentially unchanged. Since the BC contribution to IRI is unchanged, the resulting BC AAOD computed with IRI and the AERONET size distribution remains unchanged.

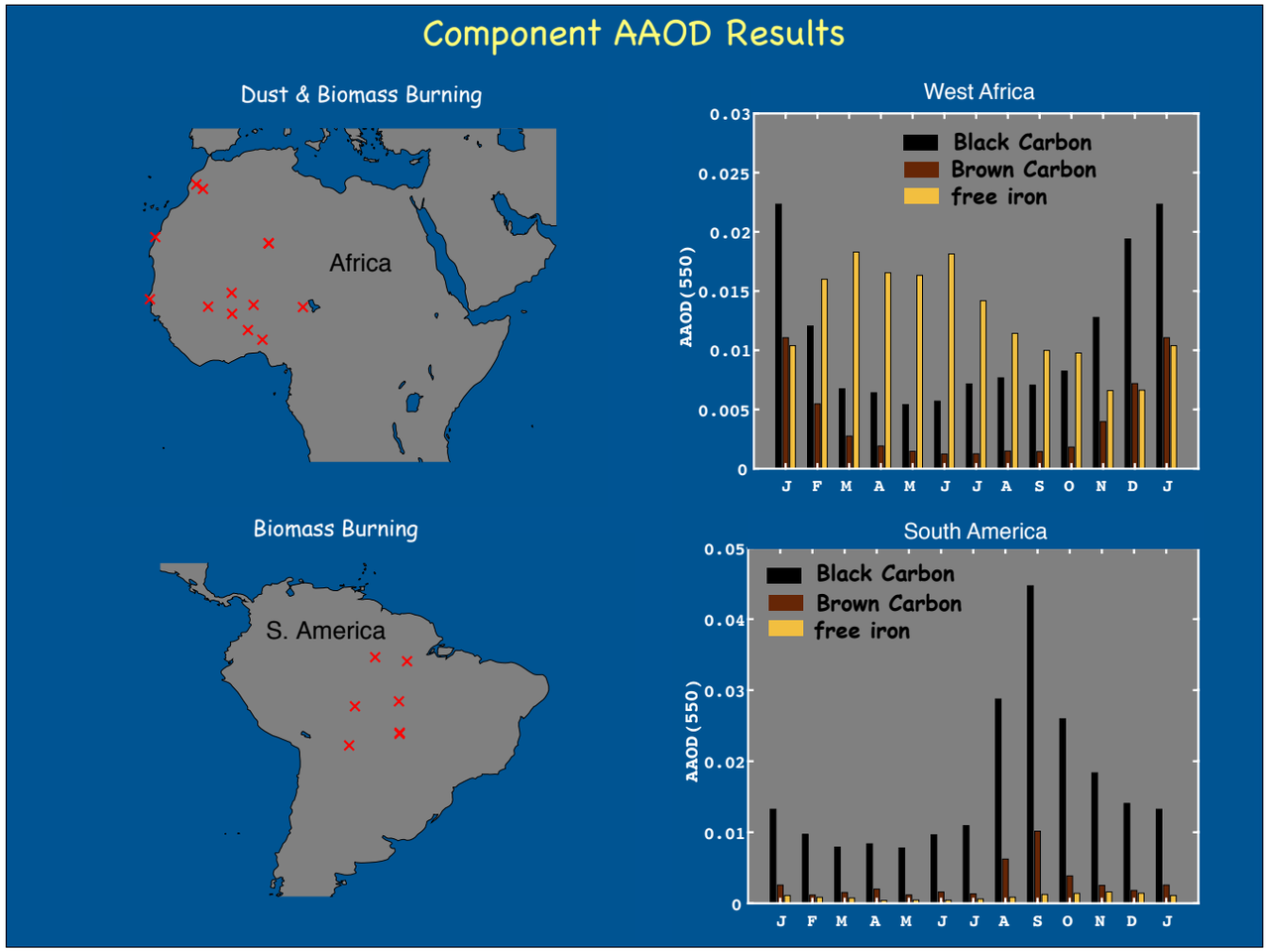

Seasonal variability of the component AAODs for BC, BrC, and Iron Oxide in two regions. The African sites clearly indicate the seasonal dust signal, which is clearly uncoupled from the seasonal carbonaceous aerosol signal (as expected). The South America sites indicate the seasonal biomass burning signal and very little dust absorption (also expected).

Conclusions

- Aerosol optical properties are not truly intrinsic (except for refractive index).
- AAE is sensitive to particle size, and should not be used without other parameters to determine BC AAOD.
- A better approach is to use complex refractive index to determine contributions of multiple aerosol components.
- Uncertainty in BC AAOD that is associated with the component AAODs in the refractive index approach is less than the AAOD measurement uncertainty.
- Most results published in *Schuster et al. (ACP, Parts 1 & 2).*

BC fractions and BC AAOD retrievals available at:

https://science.larc.nasa.gov/personal-pages/gregs/data/2019-08-26/

Acknowledgements. This material was supported by the National Aeronautics and Space Administration under the NASA Glory Science Team, issued through the Science Mission Directorate, Earth Science Division. Oleg Dubovik was supported by the Labex CaPPA project involving several research institutions in Nord-Pasde-Calais, France. Antti Arola acknowledges support from the Academy of Finland.We appreciate the efforts of the 29 AERONET and PHOTONS (Service dObservation from LOA/USTL/CNRS) principal investigators and the entire AERONET and PHOTONS teams for obtaining, processing, documenting, and disseminating their respective data sets.

APPENDIX

Effect of Size on Single-Scatter Albedo

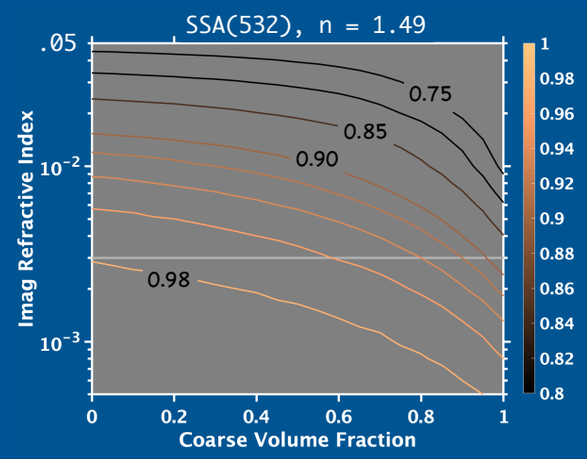

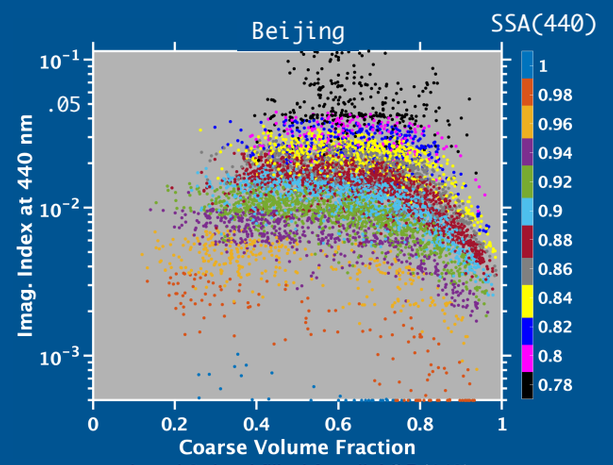

Level 2, backfilled for all AOD(440)

Bimodal Size Distribution:

$$\frac{dV}{d\ln r} = \sum_{i=1}^{2} \frac{C_{v,i}}{\sqrt{2\pi}\sigma_i} \exp\left[-\frac{(\ln r - \ln r_{v,i})^2}{2\sigma_i^2} \right]$$

$r_1 = 0.12\,\mu m$ $\quad r_2 = 3.2\,\mu m$

$\sigma_1 = 0.38$ $\quad \sigma_2 = 0.75$

Effect of Size on Lidar Ratio

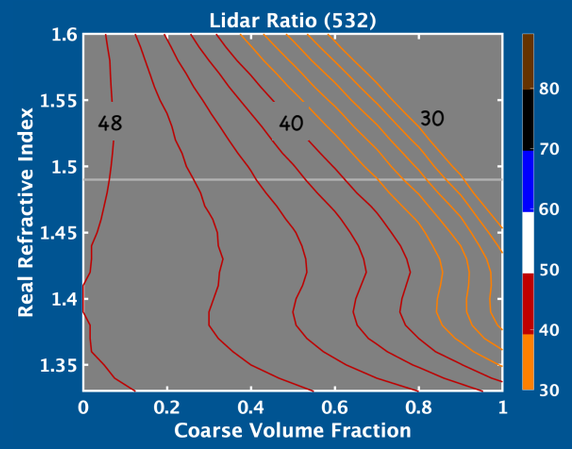

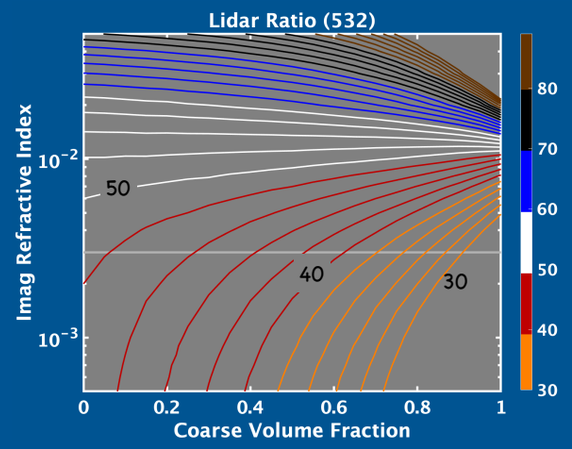

Bimodal Size Distribution:

$$\frac{dV}{d\ln r} = \sum_{i=1}^{2} \frac{C_{v,i}}{\sqrt{2\pi}\sigma_i} \exp\left[-\frac{(\ln r - \ln r_{v,i})^2}{2\sigma_i^2}\right]$$

$$r_1 = 0.12\,\mu m \qquad r_2 = 3.2\,\mu m$$
$$\sigma_1 = 0.38 \qquad \sigma_2 = 0.75$$